Introduction to the Shift Current Photovoltaic Effect

Sean Raglow

The bulk photovoltaic effect (BPVE) is a nonlinear optical effect that generates photocurrents in materials with broken inversion symmetry without the presence of an external dc electric field. This effect has garnered interest due to its potential applications in efficient solar cells. In this paper, I aim to describe the origins of the shift current photovoltaic effect, and demonstrate the process for calculating its photoresponsivity for a simple tight binding model of the 2D monochalcogenide GeS.

INTRODUCTION

The photovoltaic effect allows for the direct conversion of light to electricity is potentially the most reliable and abundant source for renewable, clean energy that exists. Traditional solar cells make us of the built in electric field within p-n junctions to separate electron/hole charge carriers and thus generate a usable photo-current. Unfortunately, the efficiency of conventional solar cells is constrained by the Shockley-Queisser limit, so exploring other processes for photo-current generation that may be able to achieve higher photo conversion efficiencies is warranted.[1] One alternative source for photo-current is the bulk photovoltaic effect (BPVE), which has been shown capable of producing an above band-gap photovoltage, may allow the Shockley-Queisser limit to be surpassed. The bulk photovoltaic effect, first discovered in the late 1960s, has several contributing components, ballistic photocurrent and shift current being the most significant. While not the focus of this paper, ballistic current is related to the violation of the "principle of detailed balancing" for photo excited non thermal carriers. Essentially, if the probability of electron transition $W_{kk'}$ from a state with moment k' to a state with momentum k' does not equal the reverse transition probability $W_{k'k}$, then there arises an asymmetry of momentum distributions. This asymmetry results in a photocurrent, but this is outside of the scope this report. Shift current arises because the real-space center of charge for valence bands differ from the center of charge for conduction bands. Thus during light-induced transitions electrons/holes shift spatially resulting in a photocurrent.[2] Most of the papers I've read claim that the dominant DC current response of the BPVE is shift current, although this is still a topic of active research, so there are some disputes about this. I will be focusing this paper on the mechanisms that lead to a shift current in materials with broken inversion symmetry.

SHIFT CURRENT

Figure 1 is very helpful for developing a qualitative sense of how shift currents arise. It shows the electron densities of GaAs for Γ electrons in the valence (a) and conduction (b) bands. Notice that these densities are spatially different. One can view this figure as a "before and after" snapshot of the positions of electrons exposed to a photoexcitation.[3] As electrons in the valence band centered around Arzenic atoms are excited, they 'shift' to be centered around a nearby Gallium atom, resulting in a current. This is complicated by different responses to different polarizations of light, and it is not clear from this analysis why the relaxation of electrons from the excited states does not simply shift them back and undo this effect. However, this suffices for a simple visualization. One paper by Liang Tan provides a simple description of the shift current from the the perspective of perturbation theory.[4] Since shift current involves carriers becoming coherently excited by incoming light (as opposed to scattering), time-dependent perturbation theory can be used to describe the electronic behavior. Thus Liang considers a three level system that is initially in a state where the $n = 0$ level is occupied, while the $n = 1, 2$ levels are unoccupied. If we expose this system to an electric field E oscillating at frequency ω, then first order time dependent perturbation gives:

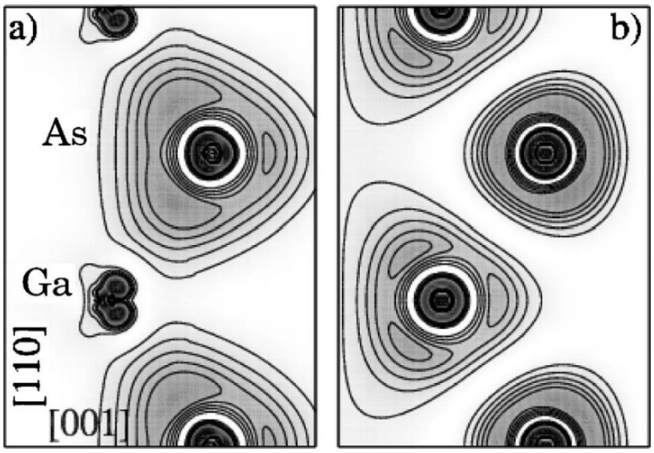

FIG. 1. A plot of the electron density in the [110] plane of GaAs. Panel (a) shows the electron density of the highest Γ valence electron, and panel (b) shows the electron density of the lowest Γ point conduction band. Source [3]

$$|\psi(t)\rangle = |\psi^0(t)\rangle + |\psi^1(t)\rangle = |0\rangle + \sum_{n\neq 0} e^{-i\omega_n t} d_n(t)\,|n\rangle \tag{1}$$

where

$$d_n(t) = -\frac{i}{\hbar} V_{n0} \left[\frac{e^{i(\omega_{n0}+\omega)t}}{i(\omega_{n0}+\omega)} + \frac{e^{i(\omega_{n0}-\omega)t}}{i(\omega_{n0}-\omega)} \right]. \quad (2)$$

Here $V_{n0} = \langle n|V|0\rangle$ is the dipole matrix element for the electric potential $V(t)$ and ω_{n0} is the energy difference between the n and 0 levels. The current carried by the state $|\psi(t)\rangle$ is given by

$$\begin{aligned} J &= \frac{e}{m} \langle \psi(t)|P|\psi(t)\rangle \\ &= \frac{e}{m} \langle \psi^1(t)|P|\psi^1(t)\rangle \\ &= \frac{e}{m} \sum_{n,n'} e^{i\omega_{n'}t} d^*_{n'}(t) e^{-i\omega_n t} d_n(t) P_{n',n} \\ &= \frac{e}{m} \sum_{n',n} g_{n',n} V^*_{n',0} V^*_{n,0} P_{n',n} \end{aligned} \quad (3)$$

Where P is the momentum operator, $P_{n',n} = \langle n'|P|n\rangle$, and $g_{n',n}$ are phases that could be calculated from 2. The key points to notice with this result is that the current is non-linear as it depends quadratically on the electric potential of the incoming light wave. This equation can be understood to say that an electron can be excited by a photon with frequency ω into the state n, or can get excited by a photon with frequency $-\omega$ into the state n'. If the interference between these two excitations is asymmetrical, then a d.c. response get be obtained, which would correspond to a situation where $V^*_{n',0} V^*_{n,0} P_{n',n}$ does not go to zero due to symmetry. An asymmetry like this would manifest in the different spatial character of the valence and conduction bands, as depicted in figure 1.

A more useful formulation for shift current can be found using response functions. if we define $E_b(\omega)$ as an electric field with frequency ω this is linearly polarized in the b direction, the the shift current takes the form

$$J_a = \sigma^{abb}(\omega) E_b(\omega) E_b(-\omega) \quad (4)$$

where a, b are Cartesian indices, and σ^{abb} is a third rank tensor, which in a D-dimension is given by

$$\sigma^{abb} = C \int \frac{dk^D}{(2\pi)^D} \sum_{n,m} f_{nm} I^{abb}_{nm} \times \delta(\omega_{nm} - \omega) \quad (5)$$

where $C = \frac{2 g_s \pi e^3}{\hbar^2}$ and $g_s = 2$ accounts for spin degeneracy.[5] n, m are band indices, $f_{nm} = f_n - f_m$ is the difference between Fermi occupations of bands n and m, and $\omega_{nm} = \omega_n - \omega_m$ is the band energy difference. From here onward, I will set $\hbar = 1$. Finally,

$$I^{abb}_{nm} = Im(r^b_{mn} r^b_{nm;a}) \quad (6)$$

where r^b_{nm} are the inter-band matrix elements of the position operator (called inter-band Berry connections[6]), which are defined as:

$$r^a_{nm} = \begin{cases} i \langle n|\partial_{k_a} m\rangle, & \text{if } n \neq m \\ 0, & \text{otherwise} \end{cases} \quad (7)$$

and $r^b_{nm;a} = \partial_{k_a} r^b_{nm} - i(\xi^a_{nn} - \xi^a_{mm}) r^b_{nm}$ are generalized derivatives of the berry connections. In the last expression $\xi^a_{nn} = i \langle n|\partial_{k_a} n\rangle$ is the diagonal berry connection for band n. These berry connections are closely related to berry phases, and can be used to calculate a variety of magnetic, optical, and electronic effects (shift current and second harmonic generation being two examples).[6] In a system with inversion symmetry, the response function σ^{abb} remains the same under an inversion operation, while the current and electric field would both pick up a negative sign. Given these properties, we can see from equation 4 that J_a must be zero in such a system. Thus only a material with broken inversion symmetry can exhibit a shift current. The derivation of expression 5for shift current can be found here[7][8].

TWO BAND MODEL

In order to calculate the shift current response of a semiconductor, it is helpful to use a generic model and write the shift current integrand I^{abb}_{nm} in terms of model parameters. Cook writes this Hamiltonian in the form

$$H = \epsilon_0 \sigma_0 + \sum_i \sigma_i f_i \quad (8)$$

where σ_0 is the identity matrix, $\sigma_i = \sigma_x, \sigma_y, \sigma_z$ are the Pauli matrices and ϵ_0, $f_i = f_x, f_y, f_z$ are unspecified functions of momentum.[5] This gives eigenvalues $E_1 = \epsilon_0 + \epsilon$, and $E_2 = \epsilon_0 - \epsilon$ corresponding to the valence and conduction bands, where $\epsilon = \sqrt{\sum_i f_i f_i}$. Evaluating equation 6 for this model requires calculating the derivatives of Bloch wave functions in order to compute the berry connections and their generalized derivatives. This is very difficult to do in practice, so to simplify the calculations, one can derive identities known as sum rules that replace wave function derivatives with sums over all the states of matrix elements of Hamiltonian derivatives.[5][8][7] The derivation is beyond the scope of this paper, but in essence by evaluating the identity

$$\partial_{k_b} \partial_{k_a} \langle n|H|m\rangle = \delta_{nm} \partial_{k_b} \partial_{k_a} E_n \quad (9)$$

one can get an expression for $r^a_{nm;b}$ in terms of derivatives of the Hamiltonian, which are much easier to compute than derivatives of Bloch functions. Plugging this expression into equation 6, with n = 1, m = 2 gives

$$I^{abb}_{12} = \frac{1}{w^{ba}_{12}} Im \left[\frac{-v^b_{221} v^a_{12} (v^b_{11} - v^b_{22})}{2\epsilon} + v^b_{21} w^{ba}_{12} \right] \quad (10)$$

where $v^b_{nm} = \langle n|\partial_{k_b} H|m\rangle$ and $w^{ba}_{nm} = \langle n|\partial_{k_b}\partial_{k_a} H|m\rangle$. To compute this expression, we would find the eigenfunctions ψ_n of the two band hamiltonian, and directly evaluate the terms to get:

$$I^{abb}_{12} = -\sum_{ijm} \frac{1}{4\epsilon^3}\left(f_m f_{i,b} f_{j,ab} - f_m f_{i,b} f_{j,a}\frac{\epsilon_{,b}}{\epsilon}\right)\epsilon_{ijm} \tag{11}$$

where $f_{i,a} = \partial_{k_a} f_i$, and $\epsilon_{,b} = \partial_{k_b}\epsilon$.

In the next section, we will follow the steps that Cook uses to calculate the shift current for a 2D material. However, they frame it in terms of the photoresponsivity tensor κ^{abb}, which is defined as the current density per incident intensity $J_a = \kappa^{abb} I_{0,b}$, where $I_{0,b} = \frac{c\epsilon_0|E_b|^2}{2}$ is the intensity for light polarized in the b direction. This is related to the σ^{abb} response function by

$$\kappa^{abb} = \frac{2\sigma^{abb}}{c\epsilon_0} \tag{12}$$

At this point, it is worthwhile to note that we have been using a fairly condensed notation, following Cook's paper since we will be using it in the next section. However, historically the response function σ^{abb} was often written in terms of the phase of the berry connections. If we let $r^b_{nm} = |r^b_{nm}|e^{i\phi^b_{nm}}$, then $I^{abb}_{nm} = |r^b_{nm}|^2 R^{ab}_{nm}$ where

$$R^{ab}_{nm} = \partial_{k_a}\phi^b_{nm} - \xi^a_{nn} + \xi^a_{mm} \tag{13}$$

is called the shift vector. The shift vector has dimensions of length, is gauge independent, and describes the change in position that occurs when an electron absorbs a photon.

All analysis thus far has been valid for thin materials that do not significantly attenuate the light as it passes through them. For thicker materials we would need to take into account an absorption coefficient.

2D TIGHT BINDING MODEL

This section is intended to give an example of the method used by Cook to compute shift current for a real material. One can make a 2D material that breaks inversion and rotational symmetry by combining a group IV and group VI element into the orthorhombic stucture of black phosphorus. GeS is predicted to be stable in such a form, and it's lattice structure is shown in figure 2[9]. Using ab initio computational techniques that are beyond the scope of this paper to approximate lattice parameters. They determined that $\vec{l}_1 = (l_1, 0)$, $\vec{l}_2 = (0, l_2)$ have parameters $l_1 = 4.53$ Å and $l_2 = 3.63$ Å, that the height difference between each zigzag was $h = 2.32$ Å, and the distance between nearest neighbor Ga and S pairs is $x_0 = 0.62$ Å. Considering only a single p_z orbital per

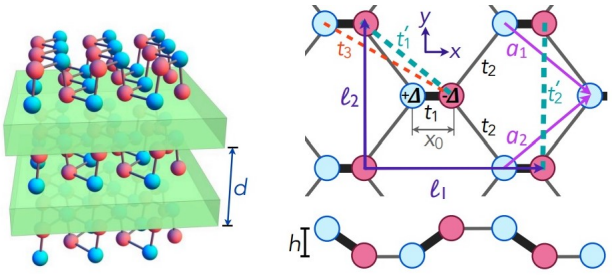

FIG. 2. The lattice structure of GeS. Source [5]

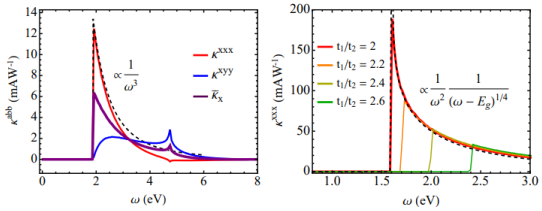

FIG. 3. Frequency dependence of the photo photoresponsivity tensor κ^{abb} for the tight binding model of GeS. The left panel shows several nonzero components of the responsivity tensor with parameters $t_1 = -2.33, t_2 = 0.61, t_3 = 0.13, \delta = 0.41$ with units of eV. $\bar{\kappa}_x = (\kappa^{xxx} + \kappa^{xyy})/2$ is the polarization averaged photoresponsivity in the x direction. The right panel shows κ^{xxx} with parameters $\delta = 0.8eV, t_3 = 0$ and different hopping ratios of $\frac{|t_1|}{t_2}$. Source [5]

site, letting δ be the on-site potential difference between nearest neighber Ge-S pairs, and letting $t_1, t_2, t_3, t_1', t_2'$ be the five hopping integrals between neighboring Ge-S, Ge-Ge, and S-S pairs Cook was able to construct a tight bonding model. Putting into the form 8, they obtain

$$\begin{aligned} \epsilon_0 &= -2t_1'(\cos(a_1\cdot k) + \cos(a_2\cdot k) - 2t_2'\cos((a_1 - a_2)\cdot k) \\ f_x + if_y &= -e^{-ix_0\cdot k}\left[t_1 + t_2\Phi(k) + t_3\Phi^*(k)\right] \\ f_z &= \delta \end{aligned} \tag{14}$$

Cook then calculates the photoresponsivity tensor for this Hamiltonian using the sum rules they derived and the various relations described in the previous section. The results are plotted as a function of frequency in figure 3, and the heat map in figure 4 shows how the photoresponsivity changes as a function of some of its hopping parameters.

For frequencies in the visible spectrum, $\omega \leq 3eV$ the total current per intensity in a conventional Si solar cell exposed to sunlight is $\approx 400\frac{mA}{W}$.[5] This is comparable to the largest values seen on the phase diagrams of figure 4. While GeS in its natural form produces far less current than this, one can imagine manipulating its properties (possibly via doping, external fields or addition of other elements into the lattice) to increase its photocurrent. Other materials with broken inversion symmetry may have even larger photoresponsivity tensors. If any

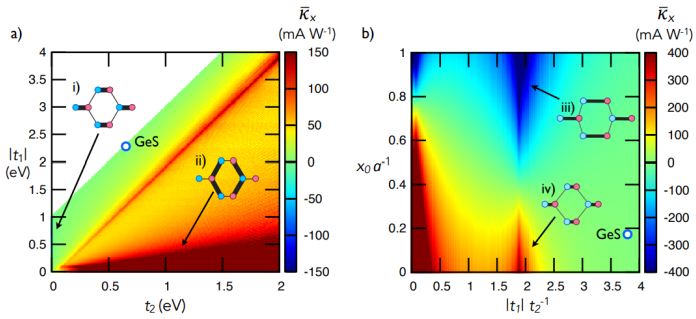

FIG. 4. Phase diagrams for monochalcogenide layer tight binding model: (a) Polarization-averaged photoresponsivity in the x-direction, $\bar{\kappa}_x$, at the band gap frequency plotted as a function of hopping parameters $|t_1|$ and t_2, keeping the band gap fixed at 1.89 eV by tuning δ accordingly. The Ge-S distance is $x_0 = -.52$ Å, and $t_3 = 0$. The location of GeS on the phase diagram is marked by a white circle with blue outline. Regions for which the gap cannot be kept at 1.89 eV are left white. (i) and (ii) show bond strengths in the limits where $|t_1| \gg t_2$ and $|t_1| \ll t_2$, respectively, to illustrate the two extremes of the phase diagram. (b) $\bar{\kappa}_x$ at the band gap frequency plotted as a function of the Ge-S distancex_0 in units of $a = (a_1^2 + a_2^2)^{1/2}$ and ratio of hopping parameters $|t_1|/t_2$. Here, δ and t_2 are set to GeS values of 1.1 eV and 0.61 eV, respectively. The location of GeS on the phase diagram is marked by a white circle with blue outline. (iii) and (iv) show two extreme cases of the phase diagram, where x0 is large and small, respectively. Source [5]

material could be found that surpasses silicon, it could profoundly change the solar energy industry.

CONCLUSION

This paper provieded an introduction to shift current as a promising mechanism for generating photo current. Since it can be generated in a homogeneous crystal lattice, without the need for a hetero structure junction, it may be possible to very cheaply produce BPVE solar cells if a suitable material is found. While we are a long ways off from developing a photovoltaic cell based on the shift BPVE that can exceed the efficiency of silicon P-N junction based photocells, the studies explored in this paper demonstrate that it is a field worth exploring.

[1] W. Shockley and H. J. Queisser, Detailed balance limit of efficiency of p-n junction solar cells, Journal of applied physics **32**, 510 (1961).

[2] J. Sipe and A. Shkrebtii, Second-order optical response in semiconductors, Physical Review B **61**, 5337 (2000).

[3] F. Nastos and J. Sipe, Optical rectification and shift currents in gaas and gap response: Below and above the band gap, Physical Review B **74**, 035201 (2006).

[4] L. Z. Tan, F. Zheng, S. M. Young, F. Wang, S. Liu, and A. M. Rappe, Shift current bulk photovoltaic effect in polar materials—hybrid and oxide perovskites and beyond, npj Comput. Mater. **2**, 1 (2016).

[5] A. M. Cook, B. M. Fregoso, F. De Juan, S. Coh, and J. E. Moore, Design principles for shift current photovoltaics, Nature communications **8**, 1 (2017).

[6] . J. M. Moura, G. B. Ventura, and R. M. Ribeiro, Berry connections calculated from first principles (2020), arXiv:2006.02744 [cond-mat.mes-hall].

[7] J. L. Hughes and J. Sipe, Calculation of second-order optical response in semiconductors, Physical Review B **53**, 10751 (1996).

[8] R. von Baltz and W. Kraut, Theory of the bulk photovoltaic effect in pure crystals, Phys. Rev. B **23**, 5590 (1981).

[9] L. C. Gomes and A. Carvalho, EnglishPhosphorene analogues: Isoelectronic two-dimensional group-iv monochalcogenides with orthorhombic structure, Physical review. B, Condensed matter and materials physics **92** (2015).